APPENDIX A

CALIBRATION AND VALIDATION OF VIDEO-BASED LUMINANCE MAPPING SYSTEM

A.1 CALIBRATION OF VIDEO-BASED LUMINANCE MAPPING SYSTEM

A.1.1 Spectral Response

The calibration of spectral response is necessary because the optical system employed in this study may or may not be the same as the human eye in terms of the spectral responses at different wavelengths. The spectral response of the video equipment was tested using a holographic spectroradiometer and calibrated by a combination of gelatin photopic filters attached at the back of the fisheye lens. For the selection of the photopic filters, the manufacturer's specification on the spectral response curve was used as the reference. Since the spectral response of the human eye is maximum at wavelength of 555 nanometers and those at other wavelengths are expressed as ratios to the maximum sensitivity, the spectral response of the camera assembly measured at 555 nanometer wavelength was used as the reference value to determine the relative spectral responses at the wavelengths of 400 nanometers through 700 nanometers. Figure A.1 shows the spectral response curves of the system with and without the photopic filters compared to the CIE relative luminous efficiency function.

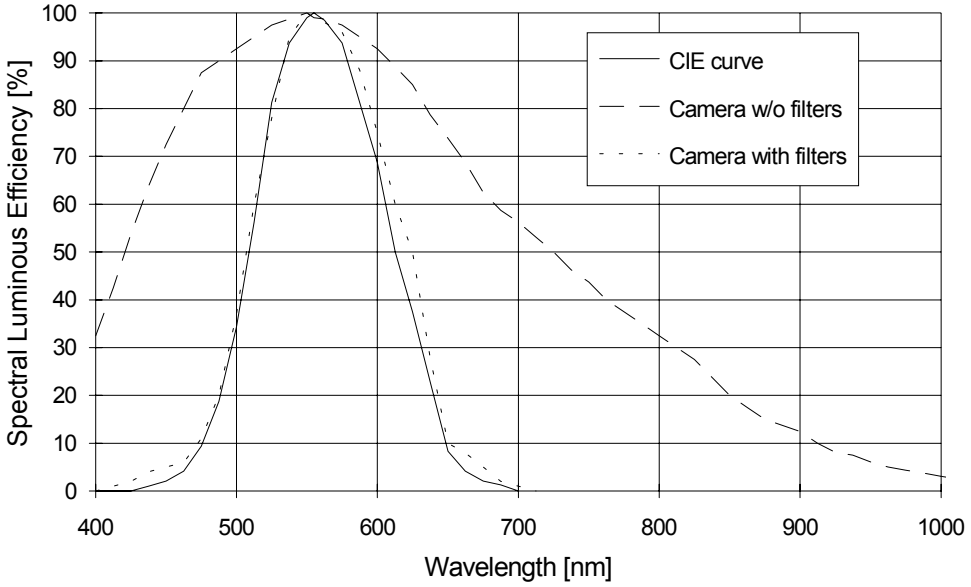

Figure A.1 Relative Spectral Luminous Efficiency

A.1.2 On-Axis System Response Function

The calibration of on-axis system response function was performed using a regulated standard lamp, the spot luminance meter, and a circular target made of a white non-specular paper. Even though the CCD sensor array is well known for its superior linearity, the output from the image capture board may have a linear or a non-linear characteristics. Figure A.2 shows the calibration setup to determine the on-axis system response function which was introduced by Rea and Jeffrey (1990). The regulated light source was placed at various distances from the target circle and both the spot luminance meter and the camera aimed and focused on the center point of the target. The locations of the lamp were determined by the luminance meter continuously measuring the luminance at the target center. When a designed luminance value was measured by the luminance meter, the movement of the lamp was stopped and the target image was captured and digitized if the CCD sensor array was not saturated by an excessive brightness of the target at a certain aperture setting of the fisheye lens. This procedure was repeated with seven different aperture settings (2.8, 4, 5.6, 8, 11, 16, and 22) of the fisheye lens. Then, the actual luminance data were plotted against the digitized pixel values to obtain the on-axis response function of the video equipment.

It was found that the functions at all seven aperture settings have nonlinear characteristics, but they were fairly well fitted by third order polynomial equations. Table A.1 summarizes the regression analysis using the least squares criteria and the maximum luminance level effective for each aperture setting in this particular system. Using these relationships, a pixel value at the optical axis can be converted to an actual luminance value (cd/m^2). Since the negative constant terms at the seven aperture settings were simply given by the least squares criteria, the luminance at a spot was set to zero when it was calculated as a negative number. Note that the absolute magnitudes of the negative constant terms at f/11 and f/22 are even larger than those of the maximum effective luminance levels at f/2.8 and f/4, respectively. Therefore, the users are required to select an aperture setting which is appropriate at a given lighting condition. Figures A.3 and A.4 show examples of the regression curves and the measured luminances plotted against the digitized pixel values at the lens aperture settings of f/4 and f/8, respectively.

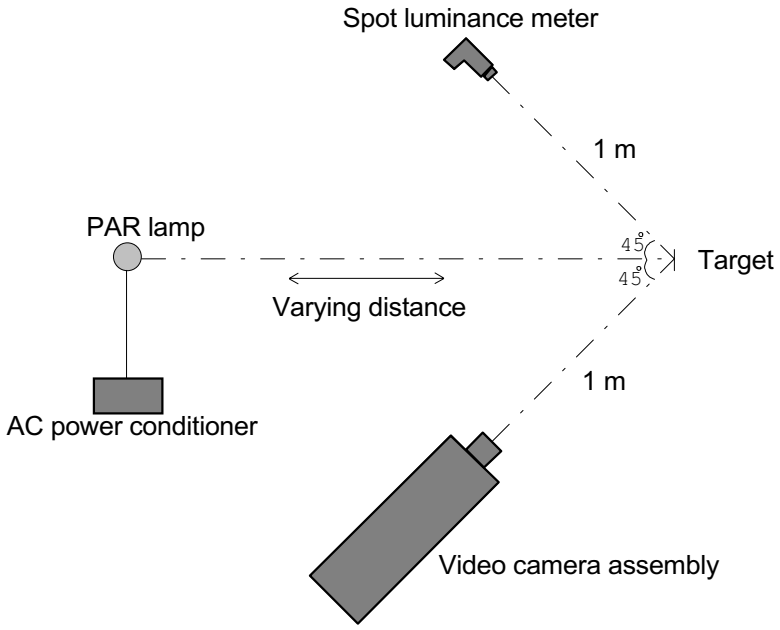

Figure A.2 Calibration Setup to Determine the On-Axis System Response Function

TABLE A.1

Regression Equations for On-Axis System Responses

f-stop	Regression Equation	R^2	Max. Lum. [cd/m²]
2.8	$L = -0.543137 + 0.081920\,P + 0.000299\,P^2 + 0.00000365\,P^3$	.9981	50
4	$L = -1.264741 + 0.191981\,P - 0.000487\,P^2 + 0.00001024\,P^3$	.9966	100
5.6	$L = -1.717727 + 0.241096\,P + 0.001075\,P^2 + 0.00000942\,P^3$	.9938	200
8	$L = -13.583269 + 1.216939\,P - 0.009138\,P^2 + 0.00005990\,P^3$	.9919	400
11	$L = -17.365726 + 1.725614\,P - 0.007869\,P^2 + 0.00007090\,P^3$	.9978	800
16	$L = -60.588432 + 5.137140\,P - 0.041910\,P^2 + 0.00023800\,P^3$	.9897	1600
22	$L = -121.211384 + 10.766132\,P - 0.100329\,P^2 + 0.00053400\,P^3$	.9884	3200

where $L =$ Target Luminance [cd/m^2]

$P =$ Digitized Pixel Value

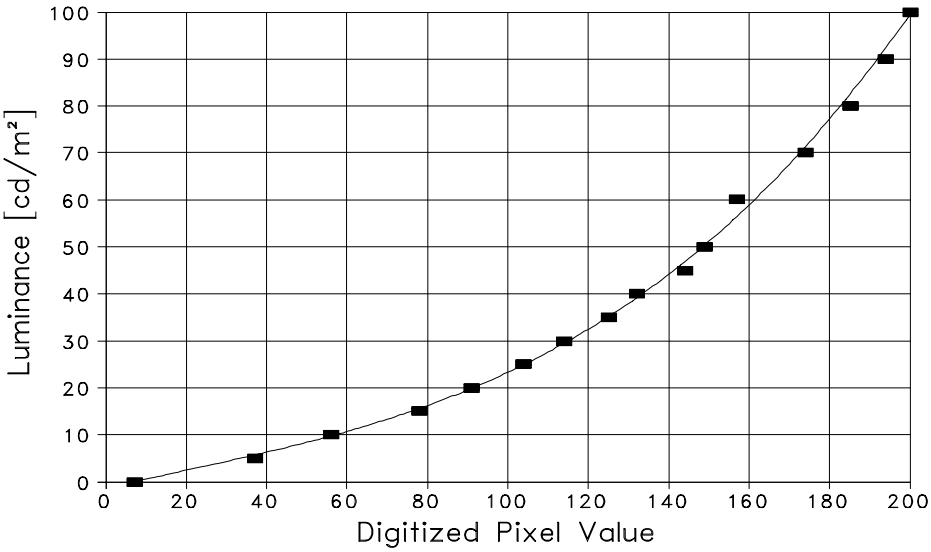

Figure A.3 On-Axis System Response Function at f/4

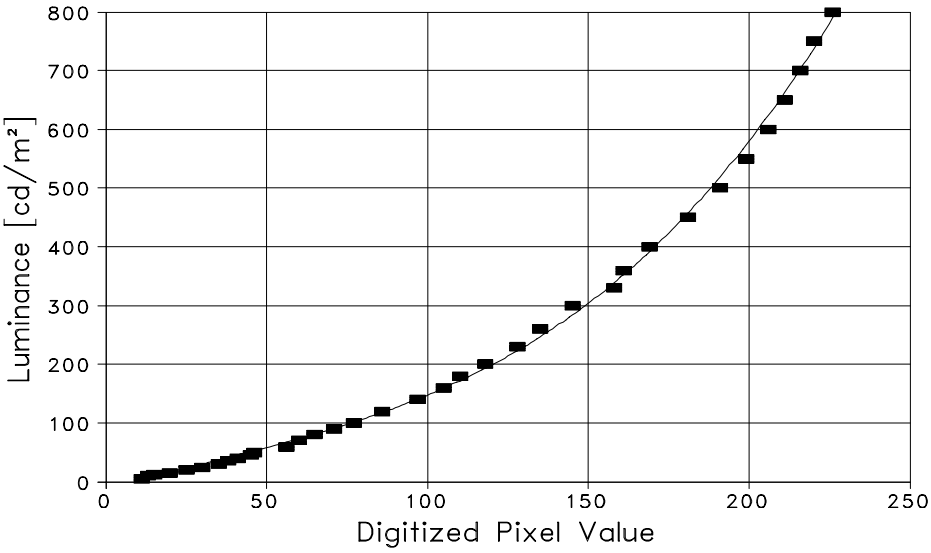

Figure A.4 On-Axis System Response Function at f/11

A.1.3 Off-Axis Luminance Transfer Function

The off-axis luminance transfer function was determined to calibrate the attenuation of light intensity away from the axis of the optical system, so called vignette effect. According to previous studies with 10 mm orthographic projection fisheye lenses (Nakamura 1976, Part 1; Weaver et al. 1986), the off-axis image illumination is flat out to about 60° from the optical axis, and then falls off approaching 90°. This non-uniformity might be attributed to the transmittance of the fisheye lens varying with the incident angles of light, reflections on the lens surface. The test was performed by capturing the interior image of an 18-inch diameter integrating sphere after a uniform luminance was measured by the spot luminance meter.

Figures A.5 and A.6 show the normalized pixel intensities at f/4 and f/11 as a function of the incident angles subtended at the optical axis. As shown in the figures, the lighting intensities detected by the CCD sensor array continuously diminished with a nonlinear pattern. The diminishing patterns at all of the seven aperture settings were well fitted by fifth order polynomial regression equations shown in Table A.2. Figures A.7 and A.8 demonstrate images before and after the off-axis luminance transfer function was corrected, respectively.

Figure A.5 Off-Axis Luminance Transfer Function at f/4

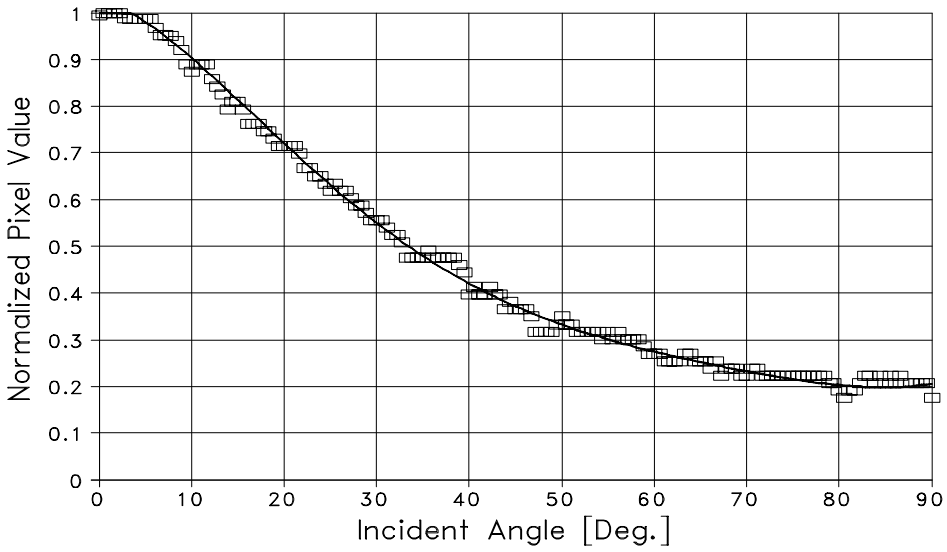

Figure A.6 Off-Axis Luminance Transfer Function at f/11

TABLE A.2

Regression Equations for Off-Axis Luminance Transfer Function

f-stop	Regression Equation	R^2
2.8	$NV = 0.993037 + 0.005747\theta - 0.000716\theta^2 + 1.2046x10^{-5}\theta^3 - 0.90\ x10^{-7}\theta^4 + 0.2640837x10^{-9}\theta^5$	0.9995
4	$NV = 0.997223 + 0.005668\theta - 0.000835\theta^2 + 1.8675x10^{-5}\theta^3 - 1.95x10^{-7}\theta^4 + 0.7838987x10^{-9}\theta^5$	0.9991
5.6	$NV = 1.016199 + 0.000852\theta - 0.000736\theta^2 + 1.6531x10^{-5}\theta^3 - 1.55x10^{-7}\theta^4 + 0.5402294x10^{-9}\theta^5$	0.9987
8	$NV = 0.993750 + 0.000483\theta - 0.000803\theta^2 + 1.6693x10^{-5}\theta^3 - 1.33x10^{-7}\theta^4 + 0.3775225x10^{-9}\theta^5$	0.9986
11	$NV = 1.032797 - 0.006846\theta - 0.000827\theta^2 + 2.4261x10^{-5}\theta^3 - 2.63x10^{-7}\theta^4 + 1.0257740x10^{-9}\theta^5$	0.9952
16	$NV = 1.066264 - 0.007527\theta - 0.000884\theta^2 + 2.6268x10^{-5}\theta^3 - 2.82x10^{-7}\theta^4 + 1.0715845x10^{-9}\theta^5$	0.9901
22	$NV = 1.020684 - 0.009512\theta - 0.000684\theta^2 + 2.1970x10^{-5}\theta^3 - 2.45x10^{-7}\theta^4 + 0.9625031x10^{-9}\theta^5$	0.9809

where NV = Normalized Pixel Value

θ = Incident Angle

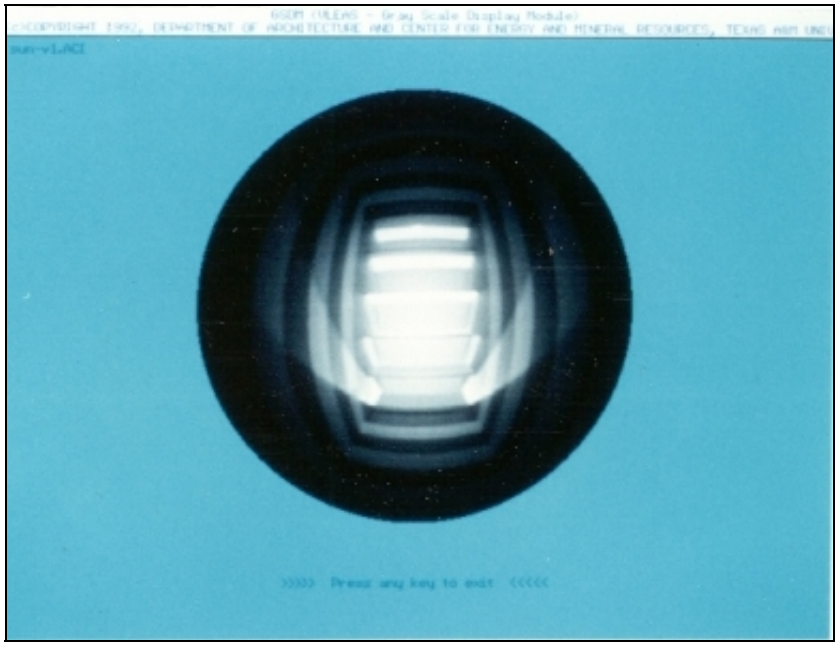

Figure A.7 Image before Off-Axis Luminance Correction

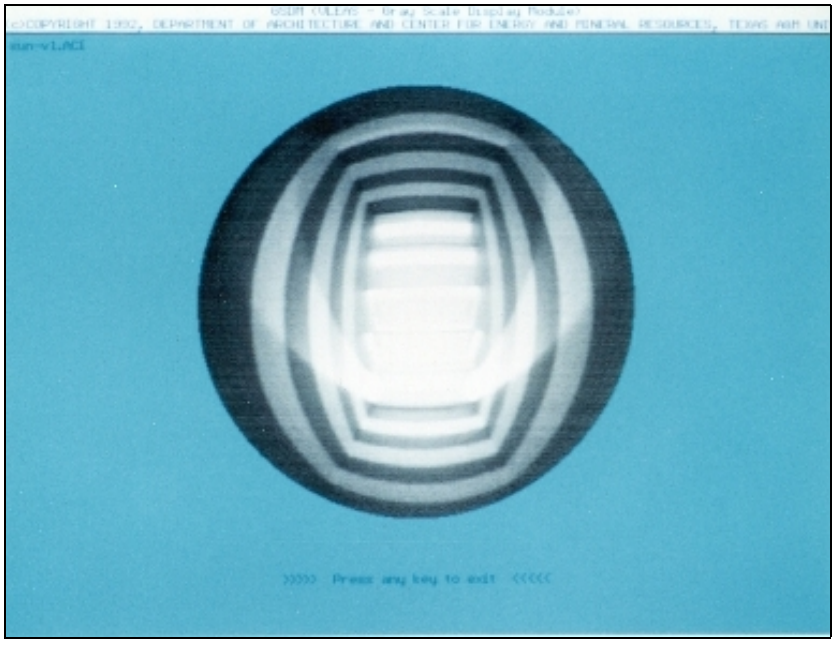

Figure A.8 Image after Off-Axis Luminance Correction

A.1.4 Geometric Accuracy Test

The geometric accuracy of the optical system was tested using a white square box with five closed surfaces measuring 200(*w*) x 200(*l*) x200(*h*) mm, in which black grid lines were evenly spaced at every 25 mm. The camera assembly was located at the edge of the opening so that its optical axis was aligned with the center point of the opposite wall in the square box. Then, the angles subtended at the optical axis by the intersections of the grid lines were calculated and compared with those read from the captured image.

The test setup and the angles geometrically calculated and read from the captured image are shown in Figure A.9. As a result, it was confirmed that the camera assembly with the equidistant projection fisheye lens and the 16 mm transfer lens faithfully captured and showed the image of 180° equidistant projection view with the maximum errors of less than ±1%. The small errors are not avoidable because a real scene is rendered on integer-based pixel locations.

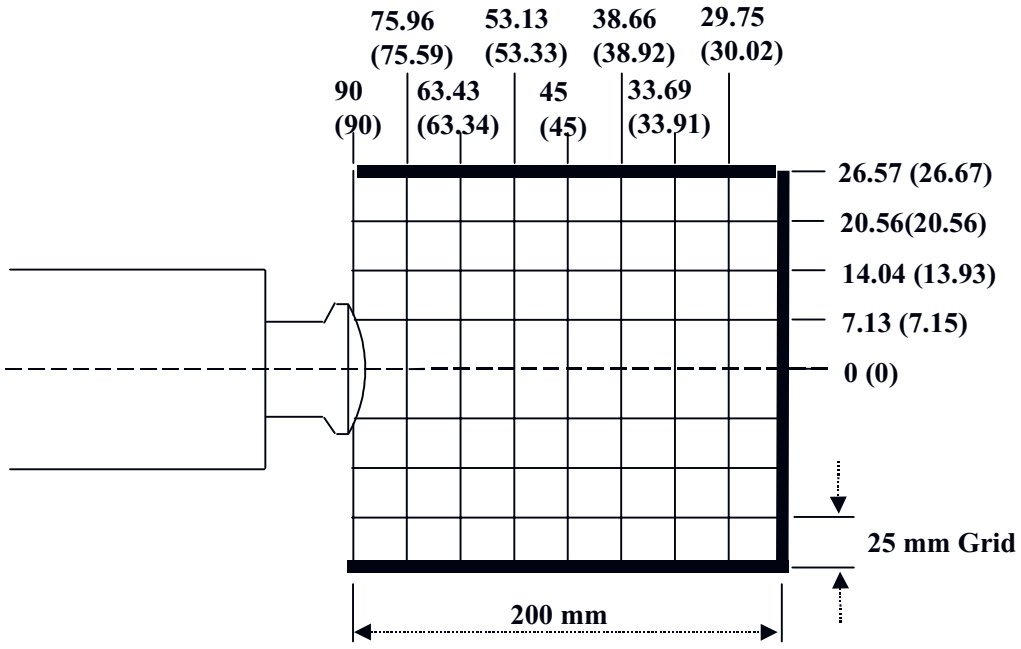

Figure A.9 Setup for Geometric Accuracy Test

A.2 VALIDATION OF VIDEO-BASED LUMINANCE MAPPING SYSTEM

As revealed in the previous sections, the geometric parameters do not require accurate mapping of surface luminances. However, the photometric parameters such as illuminance levels from windows and/or skylights require accurate mapping of surface luminances viewed from the camera positions.

The accuracy of the current system in determining the luminance and illuminance values was tested by comparing the calculated values with those measured by a spot luminance meter and a photometric sensor. The measurements were conducted inside a sky simulator at Texas A&M University. The large sky simulator measuring 8.5 m (28 ft) in diameter and 3.6m (12 ft) in height is equipped with a high intensity discharge (HID) electric lighting system as well as perimeter bands of inboard and outboard high output (HO) fluorescent lamps controlled by an integrated switching board to simulate various sky conditions.

To determine the accuracy of the current system in determining luminance, 10 cm diameter circular targets with black brims were patched on the surface of the simulated sky dome at a certain interval. Then, the luminance values determined by the current system were compared with those measured by the 1/3° precision spot luminance meter. Figure A.10 shows one of the orthographic projection images with the targets. In the figure, the point numbers of 7 through 10 were not marked because of the image compressions near the circle's edge. Figure A.11 shows the comparison of luminance values at f/5.6.

The accuracy of the current system in determining the illuminance values from the mapped pixel luminances by the previous equations were tested by comparing the calculated illuminance values with those measured by a photometric sensor inside the sky simulator. After measuring a designed level of horizontal illuminance with the photometric sensor, the sky dome image was captured when the image on the TV monitor was not saturated by extreme luminances relative to a certain aperture setting or was not too dark. Tests with horizontal illuminances higher than 7500 lux were not conducted because it was the maximum illuminance that the sky simulator could create.

Figure A.12 shows the illuminance levels determined by the current system with different aperture settings at pre-measured illuminance values. As shown in the figure, different aperture settings of the fisheye lens resulted in different calculated illuminance values and the corresponding images showed different luminance distribution figures. Since the AGC circuit of the video camera was defeated and quantity of light detected by

the image sensor array was controlled only by the aperture size of the fisheye lens, the aperture settings must be carefully decided by considering the field illuminance to obtain accurate luminance distribution figures. The appropriate aperture settings of the current system under different illuminance levels were found as shown in Table A.3. Before capturing an image, a photometric sensor should be used to measure the illuminance level at the camera position. Then, at least two different aperture settings may be tried. After obtaining an illuminance value close to the measured value, the number of pixels within a surface source and the luminance of each pixel can be used in Equation 3.15 discussed in Chapter 3 to determine illuminance levels from individual openings and certain portions of interior surfaces.

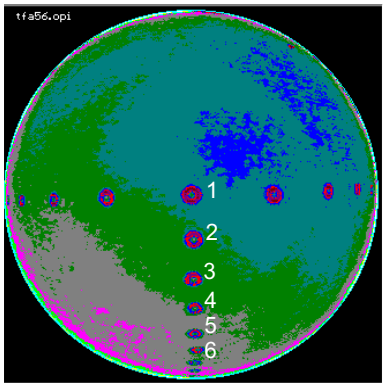

Figure A.10 Targets for Luminance Measurement

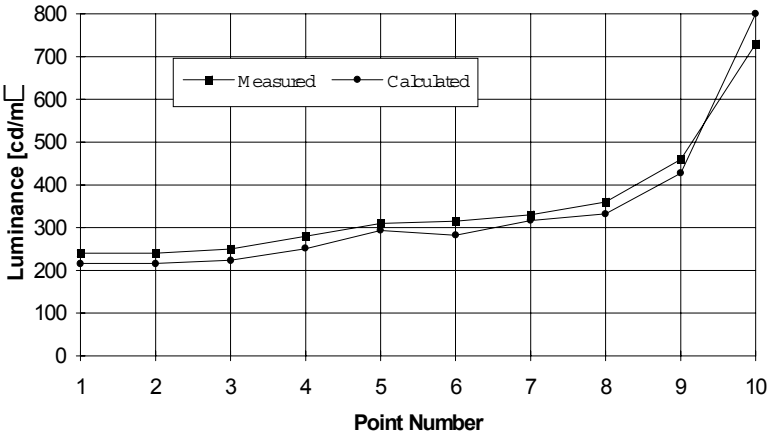

Figure A.11 Measured vs. Calculated Luminance Values (f/5.6, E_h=800 lux)

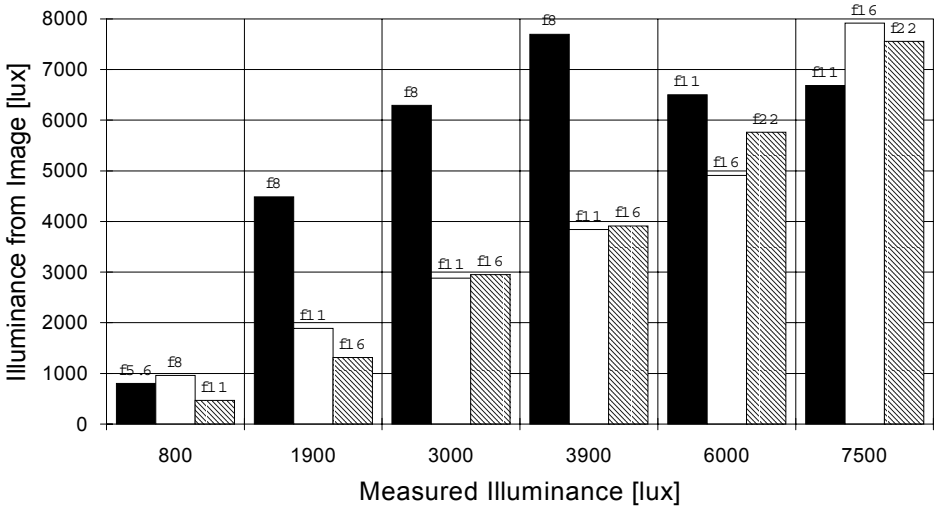

Figure A.12 Measured vs. Calculated Illuminance Values with Different Aperture Settings

TABLE A.3

Aperture Settings for Different Illuminances

Measured Illuminance [lux]	Lens Aperture
$E < 500$	f/2.8 - f/4
$500 < E < 1000$	f/5.6 - f/8
$1000 < E < 2000$	f/11
$2000 < E < 4000$	f/16
$4000 < E < 8000$	f/22

where E = horizontal or vertical (depending upon the camera position) illuminance measured by a photometric sensor.